植物学报 *Chinese Bulletin of Botany* 2021, **56** (5): 594–604, www.chinbullbotany.com
doi: 10.11983/CBB21052

·技术方法·

P515的测量原理、方法和应用

张春艳[1, 2*], 庞肖杰[2]

[1]中国科学院植物研究所公共技术中心, 北京 100093; [2]中国科学院光生物学重点实验室, 北京 100093

摘要 光谱技术已广泛应用于光合研究领域, 如光吸收信号P515和P700氧化还原动力学以及叶绿素荧光等, 可快速、准确地检测植物的光合活性。P515信号广泛存在于高等植物和藻类中, 是类囊体膜上的色素分子吸收光能后, 其吸收光谱发生位移造成。利用光诱导的P515快速和慢速动力学, 可检测PSI和PSII反应中心的比值、ATP合酶的质子传导性、围绕PSI的环式电子传递速率、质子动力势及其组分, 还可通过同步检测叶绿素荧光和P515信号研究光保护机制。该文总结了P515的主要测量原理、方法及其应用, 旨在为深入研究光合作用机理提供技术支持。

关键词 P515, ATP合酶, 环式电子传递, 质子动力势

张春艳, 庞肖杰 (2021). P515的测量原理、方法和应用. 植物学报 **56**, 594–604.

在光合作用中, 放氧光合生物吸收太阳能并裂解水分子, 在类囊体囊腔释放大量的H^+并驱动电子在膜蛋白复合物和电子载体间传递, 最终生成还原型烟酰胺腺嘌呤二核苷酸磷酸(辅酶II) (NADPH)。同时, 光合电子的传递导致质子从叶绿体基质向类囊体囊腔传递并伴随多种离子的跨膜转运, 随后卡尔文循环消耗质子进行固碳, 又导致叶绿体基质碱化, 这些因素共同诱导形成跨膜电势(ΔΨ)和质子梯度(ΔpH), 即质子动力势(proton motive force, pmf) (Cruz et al., 2001; Carraretto et al., 2016)。质子动力势驱动ATP合酶产生腺苷三磷酸(ATP), ATP和NADPH为光合作用中卡尔文循环及其它代谢途径提供能量和还原力(Kramer et al., 2003; Takizawa et al., 2007)。

在光合作用中, 类囊体膜产生的跨膜电势会改变某些光合色素的吸收光谱(Witt, 1979)。这一现象最早由Duysens (1954)发现, 小球藻(*Chlorella*)在照光条件下的吸收光谱呈双波形状且最大吸收峰在515 nm处, 即P515信号(也称ECS信号, electrochromic shift)。Junge和Witt (1968)发现, P515信号与类囊体跨膜电势呈线性关系。后来发现P515信号普遍存在于高等植物和藻类中, 即在光合作用过程中, 类囊体膜上的叶绿素b和类胡萝卜素分子吸收光能后发生能级跃迁, 而电势的产生导致能级跃迁发生改变, 从而使其吸收光谱发生位移(Fork and Amesz, 1967; Schmidt et al., 1971; Holmes et al., 1980; Hirano and Katoh, 1981; Frese et al., 2002; Zhang et al., 2009; Bailleul et al., 2010; Klughammer et al., 2013; Sukhov et al., 2016; Allorent et al., 2018; Viola et al., 2019)。

通过检测活体植物在515 nm处的吸收光谱, 可快速、无损、准确地探究2个光系统的电荷分离、质子跨膜转运和电子传递等问题。此外, P515还可与其它光谱技术结合使用, 拓展其在光合研究领域中的应用。例如, P515与叶绿素荧光联用, 可同步检测跨膜质子梯度以及质子梯度诱导产生NPQ (non-photochemical quenching), 为研究光保护的机理以及质子动力势的调控机制提供实时准确的数据。P515与P700氧化还原动力学均可计算围绕PSI的环式电子传递速率, 两者可互为印证。此外, P515与叶绿素荧光、P700氧化还原动力学结合使用, 为研究叶绿体ATP合酶的功能、环式电子传递及其调控机制、ATP/NADPH的比例分配等起到重要的技术支持。

目前, 检测P515信号的仪器主要有LED激发-探测光谱仪(JTS-10, Bio-Logic SAS, France)、双通道

收稿日期: 2021-03-23; 接受日期: 2021-06-18
基金项目: 中国科学院仪器设备功能开发技术创新项目(No.2018g0048)
* 通讯作者。E-mail: zhangchunyan@ibcas.ac.cn

调制叶绿素荧光仪(DUAL-PAM-100, Walz, Germany)和动态LED阵列差示吸收光谱仪(KLAS-100, Walz, Germany)等。LED激发-探测光谱仪可检测样品在520/540 nm的光吸收，通过在白光前放置520/540 nm的干扰滤光片可获得520/540 nm的测量光，活化光可选择绿光、橙光和红光等，可根据样品的吸收光谱选择合适的活化光。饱和闪光可由激光器提供。其它2台设备由德国Walz研发，可分别检测样品在520–550 nm和507–569 nm的差示吸收光谱，活化光可选择蓝光或红光，饱和闪光与活化光集成在同一块LED灯板上。

1 实验材料

莱茵衣藻(*Chlamydomonas reinhardtii* L.)野生型和*PGR5*突变体购自衣藻遗传中心。拟南芥(*Arabidopsis thaliana* L.)野生型为哥伦比亚生态型。

2 方法

2.1 测量PSI和PSII反应中心的比值

取2 mL暗适应并添加20%聚蔗糖的莱茵衣藻(浓度约25 μg·mL^{-1})加入比色杯，放入双通道调制叶绿素荧光仪。打开测量光(520–550 nm)，施加1次单周转饱和闪光(ST，波长635 nm，光强200 000 μmol·m^{-2}·s^{-1}，持续时间5 μs)，检测样品在520 nm处的光吸收(即P515快速动力学)。其中快速上升的幅度代表PSI和PSII反应中心的数量。样品加入二氯苯基二甲脲(DCMU)和羟胺(HA) (抑制PSII光合活性)后，同样检测P515快速动力学，其中快速上升的幅度代表PSI反应中心的数量。

2.2 测量ATP合酶的质子传导性

将暗适应3小时的拟南芥离体叶片放入双通道调制叶绿素荧光仪叶室内，活化光(波长635 nm，光强500 μmol·m^{-2}·s^{-1})照光10分钟，期间提供稳定的CO_2 (380 μmol·mol^{-1})、湿度(60%大气湿度)和温度(23°C)。关闭活化光，检测样品在黑暗250 ms的P515衰减动力学(黑暗时间可根据样品调整)，重复测量100次，取平均值。P515衰减动力学曲线半衰期的倒数反映稳态光合的质子通过ATP合酶的流出速率，即ATP合酶的质子传导率(即g_H^+，单位s^{-1})。

2.3 测量围绕PSI的环式电子传递速率

将添加20%聚蔗糖以及DCMU和HA的莱茵衣藻野生型和*PGR5*突变体(浓度约25 μg·mL^{-1})暗适应20分钟，分别检测P515快速动力学(2个样品快速上升阶段的幅度分别为1.21×10^3 ΔI/I和1.16 ×10^3 ΔI/I)。然后将莱茵衣藻野生型和*PGR5*突变体分别照光5分钟(光强约80 μmol·m^{-2}·s^{-1})，使其达到稳态光合作用，关闭活化光后分别检测其通过ATP合酶的质子流出速率，即环式电子传递速率。为方便比较，野生型质子流出速率的数据除以1.21×10^3 ΔI/I，*PGR5*突变体的数据除以1.16×10^3 ΔI/I，可将纵坐标校准为electrons/PSI，再将2组数据均一化，起点调整为0。

2.4 测量质子动力势及其组分(跨膜电势和跨膜质子梯度)

将暗适应3小时(为了降低玉米黄素的含量)的拟南芥离体叶片放入双通道调制叶绿素荧光仪叶室内，打开测量光，待基线平稳后，打开活化光(635 nm，750 μmol·m^{-2}·s^{-1})，PSII和PSI反应中心发生原初电荷分离，从而导致P515信号迅速增加。在持续照光(3 分钟)过程中，类囊体腔内不断积累的质子逐渐被流入的阴离子(主要是Cl$^-$)中和，P515信号达到相对稳态水平(Cruz et al., 2001; Schreiber and Klughammer, 2008)。活化光关闭瞬间，类囊体腔内积累的质子以不变的速率通过ATP合酶快速释放到类囊体基质，造成囊腔内阴离子过剩，从而引起信号反转，表现为P515信号迅速下降，下降的最大幅度即质子动力势(pmf)。活化光关闭后，随着类囊体腔内阴离子(主要是Cl$^-$)的外流，基质中阳离子(主要是K$^+$和Mg^{2+})内流，囊腔内外离子浓度逐渐达到平衡(Hind et al.,1974; Schönknecht et al., 1988; Pottosin and Schönknecht, 1996)，反转的P515信号又慢慢恢复，表现为信号缓慢上升并逐渐达到“暗基线”(Cruz et al., 2001; Schreiber and Klughammer, 2008)。pmf及其组分Δψ和ΔpH的计算方法依据文献(Schreiber and Klughammer, 2008)。

2.5 同步测量叶绿素荧光和P515信号

使用双通道调制叶绿素荧光仪P515/535模块和叶绿

素荧光模块，可以实现P515信号和叶绿素荧光的同步测量。将加入20%聚蔗糖的莱茵衣藻(浓度约30 μg·mL^{-1})暗适应20分钟，放入荧光仪的测量室，分别打开P515/535模块和叶绿素荧光模块的测量光，待两者信号平稳后，打开饱和闪光(635 nm, 6 000 μmol·m^{-2}·s^{-1}，持续时间250 ms)，测定黑暗状态时最大荧光产量(F_m)。之后打开活化光(635 nm, 1 500 μmol·m^{-2}·s^{-1})，PSI和PSII发生电荷分离，导致P515信号和叶绿素荧光产量均快速上升。随着强活化光持续照光，叶绿素光下最大荧光产量(F_m')下降，而P515信号达到相对稳态。活化光关闭后，F_m'逐渐恢复至最大荧光产量(F_m)，而P515信号先迅速下降至最低点，然后逐渐恢复至暗基线。

3 结果与讨论

3.1 P515信号为研究植物光适应的分子机理提供技术支持

计算2个光系统反应中心比值的常规方法是将细胞破碎后进行密度梯度离心，得到PSI和PSII的组分或者通过免疫印迹法进行定量分析，而检测P515可活体、快速地得到准确的实验结果。在毫秒级尺度内，单周转饱和闪光会诱导植物515 nm处的光吸收发生快速变化，即P515快速动力学，以此计算PSI和PSII反应中心的比值。P515快速动力学包括3个过程：快速上升阶段、缓慢上升阶段和缓慢下降阶段(图1A)。快速上升阶段指暗适应的样品，其PSI和PSII反应中心完全开放，单周转饱和闪光(ST)会诱导2个光反应中心发生原初电荷分离，从而引起515 nm处光吸收快速增加，增幅反映有活性的PSI和PSII反应中心的数量(莱茵衣藻野生型快速上升阶段的幅度为2.24×10^3 ΔI/I (图1B)。当在样品中加入DCMU和HA完全抑制PSII的光合活性后，单周转饱和闪光仅诱导PSI反应中心发生1次电荷分离，得到PSI反应中心的数量(此时莱茵衣藻野生型快速上升阶段的幅度为1.13×10^3 ΔI/I (图1B)，进而获得2个光反应中心数量的比值(约1.02)。P515信号快速上升之后有一个较慢的上升相，即慢速上升阶段，反映由原初电荷分离产生的电子在2个光系统之间的传递，与Cytb_6f处的醌循环有关。饱和闪光关闭后，由快速上升和缓慢上升阶段产生的跨

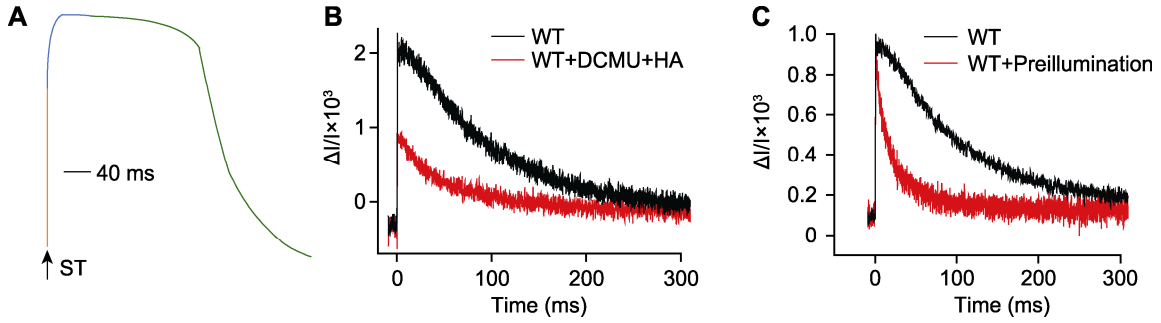

图1 饱和闪光诱导的P515快速动力学

(A) 饱和闪光诱导的P515快速动力学示意图，包括快速上升阶段(橙)、缓慢上升阶段(蓝)和缓慢下降阶段(绿)，箭头表示1次单周转饱和闪光(ST)；**(B)** 饱和闪光诱导莱茵衣藻在520–550 nm的快速吸收变化(单周转饱和闪光波长635 nm，光强200000 μmol·m^{-2}·s^{-1}，持续时间5 μs)，莱茵衣藻野生型(WT) (浓度约25 μg·mL^{-1})加入(红)和不加入(黑) 10 μmol·L^{-1}二氯苯基二甲脲(DCMU)和1 mmol·L^{-1}羟胺(HA)，测量前莱茵衣藻暗适应20分钟；**(C)** 预照光对P515快速动力学的影响，莱茵衣藻野生型在暗适应20分钟(黑)以及在光下持续照光2分钟(光强40 μmol·m^{-2}·s^{-1})，黑暗1分钟(红)后的P515快速动力学。

Figure 1 The P515 fast kinetics induced by a single turnover saturating flash

(A) The diagram of P515 fast kinetics induced by a single turnover saturating flash, rapid ascent stage (orange), slow ascent stage (blue) and slow descent stage (green), the arrow indicated a single turnover saturating flash (ST); **(B)** The rapid absorption changes of *Chlamydomonas reinhardtii* cells (WT) at 520–550 nm induced by a ST (the wavelength of ST was 635 nm, the light intensity was 200000 μmol·m^{-2}·s^{-1} and the duration was 5 μs), WT (concentration 25 μg·mL^{-1}) was incubated with (red) and without (black) 10 μmol·L^{-1} 3-(3,4-dichlorophenyl)-1,1-dimethylurea (DCMU) and 1 mmol·L^{-1} hydroxylamine (HA) for 20 min in darkness; **(C)** The affection of preillumination to the P515 fast kinetics, WT algae was incubated in darkness for 20 min (black) and preilluminated for 2 min at 40 μmol·m^{-2}·s^{-1} followed by 1 min dark (red).

膜电势消失，这是由质子通过ATP合酶外流引起(Schreiber and Klughammer, 2008; Bailleul et al., 2010; Viola et al., 2019)。

值得注意的是，饱和闪光可能会诱导PSI反应中心发生2次电荷分离，从而导致电荷分离的反应中心数量被高估(Bailleul et al., 2010)。在植物光适应的分子机理研究方面，PSI和PSII反应中心的比例关系为其研究提供了重要的数据支持，如捕光叶绿素蛋白生物合成缺陷的莱茵衣藻BF4和*p71*突变体，其PSI和PSII的天线大小均有不同程度的减小，而BF4突变体由于PSII的生物发生受阻，导致PSI/PSII反应中心比例增加至1.25 (Bujaldon et al., 2020)。虽然PSI和PSII的天线大小未发生改变，但莱茵衣藻还可通过降低PSI/PSII反应中心的比值适应强光变化(Bonente et al., 2012)。缺失质体蓝素(PC)的莱茵衣藻突变体在状态转换过程中可达到完全的状态1，其PSI/PSII比值比野生型下降10% (Nawrocki et al., 2016)。

该测量过程易受预照光的影响，应确保样品在测量前处于完全黑暗状态。预照光会启动光合作用，导致部分反应中心发生电荷分离，驱动电子在光合膜上传递，从而使饱和闪光诱导的快速上升幅度降低，缓慢上升阶段消失(图1C) (Schreiber and Klughammer, 2008; Alric, 2014)。此外，预照光会激活类囊体膜上的ATP合酶，增加膜的H^+传导性，从而导致缓慢下降阶段显著加快，因此通过缓慢下降阶段的衰减速率可判断类囊体膜的通透性(Schreiber and Klughammer, 2008)。

饱和闪光诱导的P515快速动力学曲线的原始信号以伏特为单位记录，为将P515信号放大，可通过校正程序将其转换成ΔI/I单位。以图1B为例，在莱茵衣藻野生型中加入DCMU和HA后，快速上升阶段的幅度为1.13×10^3 ΔI/I，代表饱和闪光仅诱导PSI反应中心发生1次电荷分离，产生1个电子，即1 electron/PSI。为方便比较，P515快速动力学曲线数据除以PSI进行1次电荷分离的幅度，可将纵坐标校准为每个PSI传递的电子数，即electrons/PSI。

3.2 P515信号为研究叶绿体ATP合酶的功能提供技术支持

当植物处于稳态的光合作用时，通过光合电子传递引起的质子流入类囊体囊腔的速率与通过ATP合酶的质子流出速率相等(Sacksteder and Kramer, 2000)。DIRK (dark internal relaxation kinetics)技术是利用短暂的黑暗(<500 ms)干扰处于稳态光合的电子和质子流，检测样品在520 nm处的光吸收(Sacksteder et al., 2000)。该方法可估算叶绿体ATP合酶的活性(Cruz et al., 2001)。其原理是当ATP合酶活性降低时，通过ATP合酶的质子流出速率也会相应降低。拟南芥野生型在500 μmol·m^{-2}·s^{-1}的光照强度下，叶绿体ATP合酶的质子传导率(g_H^+)为94.3·s^{-1} (图2)。拟南芥*bfa1*和*bfa3*是两个ATP合酶突变体，在不同光照强度下，其g_H^+分别下降至野生型的30%和50%，同时均表现出较高的NPQ (Zhang et al., 2016, 2018)。这是因为当ATP合酶活性降低时，通过ATP合酶的质子流出效率降低，导致质子在类囊体囊腔累积，囊腔过度酸化会抑制NPQ衰减，从而表现出高水平的NPQ。烟草(*Nicotiana tabacum*) GTG-atpB突变体的g_H^+降至

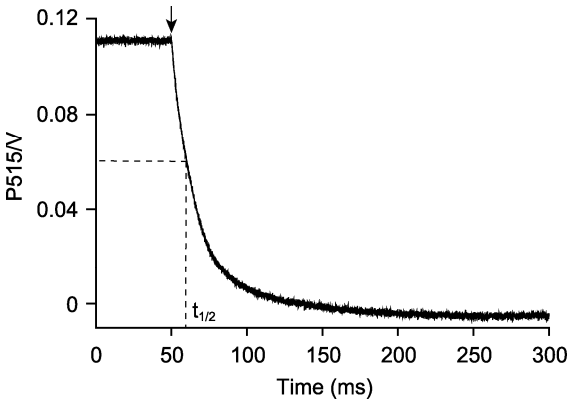

图2 测量拟南芥叶绿体ATP合酶的质子传导性

拟南芥离体叶片在光强为500 μmol·m^{-2}·s^{-1}的活化光(635 nm)下照光10分钟，照光期间提供稳定的CO_2 (380 μmol·mol^{-1})、湿度(60%大气湿度)和温度(23°C)。检测黑暗250 ms的P515衰减动力学，重复100次后取平均值。ATP合酶的质子传导率为P515衰减动力学曲线半衰期($t_{1/2}$)的倒数，即94.3·s^{-1}。箭头表示活化光关闭。

Figure 2 Detection the H^+ conductivity of chloroplast ATP synthase in *Arabidopsis thaliana*

The detached leaf of *Arabidopsis thaliana* was exposed to light (635 nm, 500 μmol·m^{-2}·s^{-1}) for 10 min, and provided stable CO_2 (380 μmol·mol^{-1}), humidity (60% atmospheric humidity) and temperature (23°C) during illumination. Detected the P515 decay kinetics curve in darkness that lasted 250 ms, the curve corresponded to 100 independent biological replicates. The H^+ conductivity of ATP synthase was 94.3·s^{-1}, which is the reciprocal of the half-time ($t_{1/2}$) of P515 decay kinetics curve. The arrow indicated light off.

野生型的25%, 且突变体的碳同化能力、线式电子传递速率和$P700^+$再还原能力也显著降低(Rott et al., 2011)。P515与叶绿素荧光、P700氧化还原动力学的结合使用在烟草、玉米(*Zea mays*)、拟南芥和豌豆(*Pisum sativum*)等叶绿体ATP合酶突变体的表型筛选和功能研究方面发挥了重要作用(Rott et al., 2011; Zoschke et al., 2012; Fristedt et al., 2015; Sukhov et al., 2016; Zhang et al., 2016)。

3.3 P515信号为研究环式电子传递及调控机制提供技术支持

在高等植物和真核藻类中存在线式(LEF)和环式(CEF) 2种电子传递途径, 环式电子传递对光合作用的功能调控已成为研究热点(Joliot and Joliot, 2002; Wang et al., 2006; Lucker and Kramer, 2013; Takahashi et al., 2013; Alric, 2014)。目前检测CEF的常用方法是将PSII光合活性抑制后(加入DCMU和HA), 通过$P700^+$的再还原速率计算环式电子传递速率。上文提到利用DIRK技术可测量通过ATP合酶的质子流出速率, 而该速率等于光驱动的通过PSI和PSII的总电子传递速率(Joliot and Joliot, 2002)。因此, 将PSII光合活性抑制后, 通过ATP合酶的质子外流速率等于围绕PSI的环式电子传递速率。已有研究表明, 将莱茵衣藻PSII光合活性抑制后, P515与P700氧化还原动力学检测到的围绕PSI的环式电子传递速率呈线性关系(Lucker and Kramer, 2013; Alric, 2014)。

Alric (2014)研究发现, 经DCMU和HA处理后莱茵衣藻野生型的PSI在70 ms时传递了1个电子, 光化学速率为$14 \cdot s^{-1}$ ($1/70 \times 10^{-3}$ s), 即环式电子传递速率为$14\ e^- \cdot s^{-1} \cdot PSI^{-1}$。此外, *PGR5*突变体的环式电子传递速率与野生型相比变化不大, 说明莱茵衣藻中NDA2 (type II NADPH dehydrogenase)介导的环式电子通路可能优于或者可替代PGR5通路, 这也与我们的实验结果一致(图3)。但当莱茵衣藻野生型和*PGR5*突变体在厌氧环境且加入DCMU处理后, PGR环式电子通路可能被激活, 导致野生型的环式电子传递速率明显增大, 达到$66\ e^- \cdot s^{-1} \cdot PSI^{-1}$ (15 ms传递1个电子), 而*PGR5*突变体的环式电子传递速率变化不大(Tolleter et al., 2011; Alric, 2014)。

当植物受到环境胁迫时, 环式电子传递的主要作用可能是通过增加ATP的供给保障光合作用高效运行(Kramer et al., 2004; Nandha et al., 2007)。例如, 当烟草受到热胁迫且CO_2同化受阻时, NDH (NAD(P)H dehydrogenase)介导的环式电子传递会被快速激活, 从而启动环式光合磷酸化产生ATP (Wang et al., 2006)。由于ATP与NADPH的产生和消耗紧密相关, 因此围绕PSI的环式电子传递可平衡ATP与NADPH的比值(Kramer and Evans, 2011)。例如, 在低浓度无机碳条件下, 莱茵衣藻可能通过增大环式电子传递速率满足对ATP/NADPH增加的需求(Lucker and Kramer, 2013)。该方法的缺点是样品经过DCMU等抑制剂处理后, 会影响细胞内的氧化还原状态或者代谢状态, 这些因素可能会激活CEF的调控机制, 进而影响CEF检测的准确性(Lucker and Kramer, 2013)。在不使用PSII抑制剂的条件下, 可利用g_H^+与

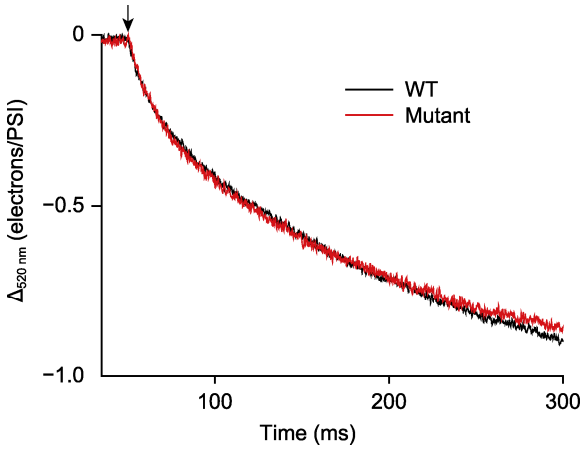

图3 测量莱茵衣藻围绕PSI的环式电子传递速率

莱茵衣藻野生型(WT)和*PGR5*突变体(Mutant)在光强为80 μmol·m^{-2}·s^{-1}的活化光(635 nm)下照光5分钟, 关光后检测围绕PSI的环式电子传递速率, 黑暗持续时间为250 ms。测量前, 藻细胞(浓度约25 μg·mL^{-1})加入10 μmol·L^{-1}二氯苯基二甲脲(DCMU)、1 mmol·L^{-1}羟胺(HA)和20%的聚蔗糖, 暗适应20分钟。箭头表示活化光关闭。

Figure 3 Detection the cyclic electron flow rate around photosystem I in *Chlamydomonas reinhardtii*

The *C. reinhardtii* cells (WT) and *PGR5* mutant (Mutant) were exposed to light (635 nm, 80 μmol·m^{-2}·s^{-1}) for 5 min. The cyclic electron flow rate was detected after the light was turned off and the darkness duration was 250 ms. Before measurement, algal cells (about 25 μg·mL^{-1}) were incubated with 10 μmol·L^{-1} 3-(3,4-dichlorophenyl)-1,1-dimethylurea (DCMU), 1 mmol·L^{-1} hydroxylamine (HA) and 20% ficoll for 20 min in darkness. The arrow indicated light off.

线式电子传递速率的比值估算环式电子的相对传递速率，其中线式电子传递速率可通过叶绿素荧光检测PSII的光化学量子产量，该量子产量乘以光强得到。该方法的优点是不会破坏样品正常的生理状态(Sacksteder and Kramer, 2000; Joliot and Joliot, 2002; Baker et al., 2007; Lucker and Kramer, 2013)。

3.4 P515信号为研究质子动力势及调控机制提供技术支持

P515分钟级的慢速动力学比较复杂，既反映质子动力势的生成，也反映玉米黄素的生成。质子动力势(proton motive force, pmf)驱动ATP合酶产生ATP，而pmf的组分——ΔpH会诱导光保护机制，将过剩的光能以热能的形式耗散，保护PSII免受光损伤(Niyogi et al., 1998; de Bianchi et al., 2010; Checchetto et al., 2013, 2016)，还可通过降低电子在Cytb_6f复合物的传递速率，保护PSI免受光抑制(Sonoike, 2011; Yamori et al., 2011)。跨膜电势(ΔΨ)也可调节PSII的光损伤。研究发现，高水平的ΔΨ不仅降低NPQ的诱导效率(Duan et al., 2016)、增加PSII的光敏感性(Davis et al., 2016)，还导致PSII反应中心发生电荷重组，促使单线态氧水平升高，造成严重的光损伤(Bennoun, 1994)。我们的研究结果显示，拟南芥在100 μmol·m^{-2}·s^{-1}的光强下，pmf为1.3，ΔpH约占56%，而当光强达到750 μmol·m^{-2}·s^{-1}时，pmf增至7.2，ΔpH所占比例增至68%，ΔΨ减少至32% (图4)，说明ΔpH可能在光保护中起更关键的作用。

虽然ΔpH和ΔΨ在质子动力势中的分配机制还不清楚，但是多种离子通道或转运蛋白参与调节两个组分的分配，进而影响光合效率(Checchetto et al., 2013, 2016; Davis et al., 2017; Spetea et al., 2017)。例如，双孔K$^+$通道蛋白TPK3缺失的拟南芥突变体，由于K$^+$外排受阻导致ΔpH的形成受损，同时NPQ诱导效率降低(Carraretto et al., 2013); Cl$^-$通道蛋白AtBest缺失会导致拟南芥pmf和ΔΨ水平显著升高，说明Cl$^-$向囊腔内的转运可消散ΔΨ，从而调控pmf的分配(Duan et al., 2016)。

3.5 P515信号和叶绿素荧光同步测量为研究光保护机制提供新方法

植物体内存在多种能量耗散机制，如叶绿素荧光淬灭和热耗散。这些能量耗散机制可能均受类囊体腔酸

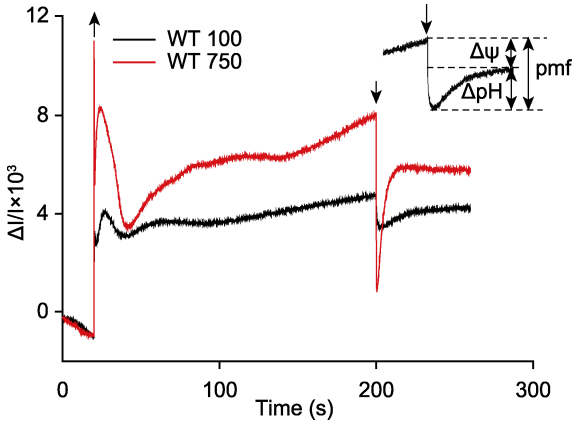

图4 拟南芥质子动力势(pmf)及其组分(ΔΨ和ΔpH)的测定
拟南芥离体叶片在光强为100 μmol·m^{-2}·s^{-1} (WT 100，黑)和750 μmol·m^{-2}·s^{-1} (WT 750，红)的活化光(635 nm)下照光3分钟，照光期间提供稳定的CO_2 (380 μmol·mol^{-1})、湿度(60%大气湿度)和温度(23°C)。黑暗时间60秒，曲线为3次重复的平均值。测量前，拟南芥叶片暗适应至少3小时。向上箭头表示活化光打开，向下箭头表示活化光关闭。

Figure 4 Detection the proton motive force (pmf) and its two components (Δψ and ΔpH) in *Arabidopsis thaliana*
The detached leaf of *Arabidopsis thaliana* was exposed to light (635 nm, 100 μmol·m^{-2}·s^{-1}, labeled as WT 100, black and 750 μmol·m^{-2}·s^{-1}, labeled as WT 750, red) for 3 min, and provided stable CO_2 (380 μmol·mol^{-1}), humidity (60% atmospheric humidity) and temperature (23°C) during illumination. The dark time was 60 s and the curve corresponded to 3 independent biological replicates. The *Arabidopsis* leaf was darkly adapted for at least 3 hours before measurement. The up arrow indicated light on, and the down arrow indicated light off.

化的调控(付振书等，2004)，同步检测活体样品在正常/高光胁迫条件下的P515信号与叶绿素荧光，可得到实时准确的同步变化数据，有利于分析各能量耗散机制之间的关系，深入研究光保护机理。莱茵衣藻是研究光合作用的模式生物，用强活化光(1 500 μmol·m^{-2}·s^{-1})处理莱茵衣藻时，会导致大部分光合反应中心关闭，光化学量子产量降低，对光合膜有害的过剩激发能量累积。此外，光合电子传递将质子从类囊体基质不断转移到类囊体囊腔，从而使类囊体囊腔不断酸化，逐渐建立pmf，与此同时激活非光化学猝灭(NPQ) (Demmig-Adams et al., 2012)。在莱茵衣藻中，NPQ依赖于一种色素结合蛋白-光捕获蛋白(LHCSR)，该蛋白具有pH敏感性。LHCSR的C端结构域暴露在类囊体囊腔侧，随着类囊体囊腔的不断酸

化，NPQ被激活，从而耗散过剩的激发能，启动光保护机制(Liguori et al., 2013)。随着强活化光的持续照光，类囊体囊腔内外离子浓度逐渐平衡，pmf达到最大值。活化光关闭后，类囊体腔内积累的质子通过ATP合酶快速释放到基质，囊腔酸化程度降低，NPQ逐渐衰减至最低水平，表现为P515信号先迅速下降至最低点，然后不断恢复至暗基线，而叶绿素荧光产量F_m'不断恢复至最大荧光产量(F_m) (图5)。由于P515信号比较灵敏，受外界环境影响较大，测量时可能会出现错误的信号，分析数据时需要更加仔细。

3.6 P515信号的局限性

P515是光谱技术，正确解析P515光谱信号非常关键。在光谱检测过程中，类胡萝卜素三体的形成与降解会引起515 nm的光谱变化，从而造成信号重叠(Kramer and Mathis, 1980)。高等植物和绿藻在照光

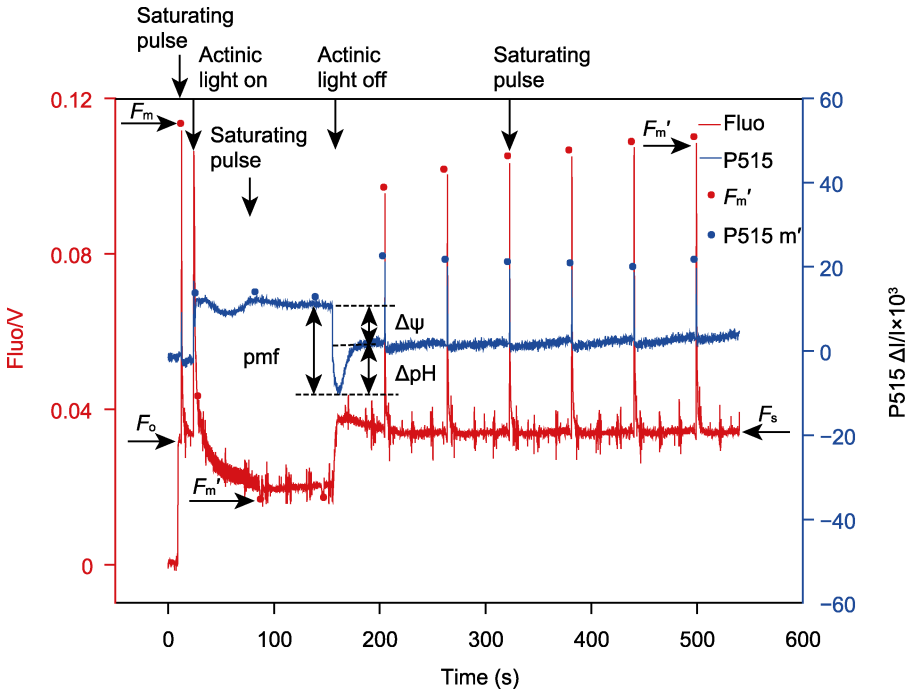

图5 同步测量莱茵衣藻P515信号和叶绿素荧光

将莱茵衣藻野生型(浓度约30 μg·mL^{-1})暗适应20分钟，放入荧光仪的测量室，分别打开P515/535模块和叶绿素荧光模块的测量光，测定初始荧光产量(F_o)。打开饱和闪光(635 nm, 6000 μmol·m^{-2}·s^{-1}，持续时间250 ms)，测定黑暗状态下的最大荧光产量(F_m)。之后打开活化光(635 nm, 1500 μmol·m^{-2}·s^{-1})，持续照光140秒，期间每隔60秒施加1次饱和闪光，测定光下最大荧光产量(F_m')。活化光关闭后测定质子动力势(pmf)及其组分(ΔΨ和ΔpH)，与此同时每隔60秒施加1次饱和闪光，检测黑暗状态下的荧光产量是否恢复到最大荧光产量(F_m)。F_o: 初始荧光产量; F_m: 最大荧光产量; F_m': 光下最大荧光产量; F_s: 稳态荧光产量; Actinic light: 活化光; Saturating pulse: 饱和闪光; pmf: 质子动力势; ΔΨ: 跨膜电势; ΔpH: 跨膜质子梯度

Figure 5 Simultaneous measurement of the P515 signal and fluorescence in *Chlamydomonas reinhardtii*

The *C. reinhardtii* cells (WT, about 30 μg·mL^{-1}) were placed in the chamber of the chlorophyll fluorometer after dark adaptation for 20 minutes. The measuring lights of the P515/535 module and the chlorophyll fluorescence module were turned on respectively to determine the original fluorescence yield (F_o). Then a saturating pulse (635 nm, 6000 μmol·m^{-2}·s^{-1}, duration 250 ms) was turned on to detect the maximal fluorescence yield (F_m) in darkness. Then an actinic light (635 nm, 1500 μmol·m^{-2}·s^{-1}) was turned on for 140 seconds, during which a saturating flash was applied every 60 seconds to detect the maximum fluorescence yield (F_m') under light. The proton motive force (pmf) and its components (ΔΨ and ΔpH) were measured after the actinic light was turned off, meanwhile a saturating pulse was applied every 60 seconds to check whether the fluorescence yield was restored to the maximum fluorescence yield (F_m) in darkness. F_o: Original fluorescence yield; F_m: Maximal fluorescence yield; F_m': Maximal fluorescence yield under light; F_s: Steady state fluorescence yield; pmf: Proton motive force; ΔΨ: Transmembrane potential; ΔpH: Transmembrane proton gradient

过程中会引起玉米黄素吸收峰的红移, 造成535 nm的光谱变化, 该信号也参与ΔpH的建立(Ruban et al., 2002)。虽然P515信号已在高等植物和绿藻中被广泛使用, 但是在蓝细菌(*Synechococcus elongatus*)、红藻(*Cyanidioschyzon merolae*)和硅藻(*Chaetoceros gracilis*)等物种的应用非常少, 这主要受限于P515光谱信号的正确解析。此外, 前文提及的P515测量方法中存在一些因素也会影响P515检测的准确性。例如, 饱和闪光诱导的PSI反应中心发生电荷分离的次数以及在测量过程中使用的抑制剂等。

相比高等植物稳定的P515光谱信号, 悬浮绿藻受外界环境的影响较大, 不同培养批次藻细胞的P515光谱信号重复性差。为保证藻细胞处于最佳的生理状态, 可先用叶绿素荧光技术快速检测细胞的光合活性是否正常, 再进行P515信号检测。此外, 在绿藻中加入10%–20%的聚蔗糖, 可有效降低藻细胞的沉降, 从而达到较好的重复性。

致谢 感谢中国科学院植物研究所温晓刚研究员、黄芳研究员、田利金研究员和中国科学院分子植物科学卓越创新中心(植物生理生态研究所)米华玲研究员在文章撰写过程中提出的宝贵意见。

参考文献

付振书, 赵世杰, 孟庆伟 (2004). 类囊体腔的酸化与过剩激发能耗散. 植物学通报 **21**, 486–494.

Allorent G, Byrdin M, Carraretto L, Morosinotto T, Szabo I, Finazzi G (2018). Global spectroscopic analysis to study the regulation of the photosynthetic proton motive force: a critical reappraisal. *Biochim Biophys Acta Bioenerg* **1859**, 676–683.

Alric J (2014). Redox and ATP control of photosynthetic cyclic electron flow in *Chlamydomonas reinhardtii*: (II) involvement of the PGR5-PGRL1 pathway under anaerobic conditions. *Biochim Biophys Acta Bioenerg* **1837**, 825–834.

Bailleul B, Cardol P, Breyton C, Finazzi G (2010). Electrochromism: a useful probe to study algal photosynthesis. *Photosynth Res* **106**, 179–189.

Baker NR, Harbinson J, Kramer DM (2007). Determining the limitations and regulation of photosynthetic energy transduction in leaves. *Plant Cell Environ* **30**, 1107–1125.

Bennoun P (1994). Chlororespiration revisited: mitochondrial-plastid interactions in *Chlamydomonas*. *Biochim Biophys Acta Bioenerg* **1186**, 59–66.

Bonente G, Pippa S, Castellano S, Bassi R, Ballottari M (2012). Acclimation of *Chlamydomonas reinhardtii* to different growth irradiances. *J Biol Chem* **287**, 5833–5847.

Bujaldon S, Kodama N, Rathod MK, Tourasse N, Ozawa SI, Sellés J, Vallon O, Takahashi Y, Wollman FA (2020). The BF4 and p71 antenna mutants from *Chlamydomonas reinhardtii*. *Biochim Biophys Acta Bioenerg* **1861**, 148085.

Carraretto L, Formentin E, Teardo E, Checchetto V, Tomizioli M, Morosinotto T, Giacometti GM, Finazzi G, Szabó I (2013). A thylakoid-located two-pore K^+ channel controls photosynthetic light utilization in plants. *Science* **342**, 114–118.

Carraretto L, Teardo E, Checchetto V, Finazzi G, Uozumi N, Szabo I (2016). Ion channels in plant bioenergetic organelles, chloroplasts and mitochondria: from molecular identification to function. *Mol Plant* **9**, 371–395.

Checchetto V, Teardo E, Carraretto L, Formentin E, Bergantino E, Giacometti GM, Szabo I (2013). Regulation of photosynthesis by ion channels in cyanobacteria and higher plants. *Biophys Chem* **182**, 51–57.

Checchetto V, Teardo E, Carraretto L, Leanza L, Szabo I (2016). Physiology of intracellular potassium channels: a unifying role as mediators of counterion fluxes? *Biochim Biophys Acta Bioenerg* **1857**, 1258–1266.

Cruz JA, Sacksteder CA, Kanazawa A, Kramer DM (2001). Contribution of electric field (Δψ) to steady-state transthylakoid proton motive force (pmf) *in vitro* and *in vivo*. Control of pmf parsing into Δψ and ΔpH by ionic strength. *Biochemistry* **40**, 1226–1237.

Davis GA, Kanazawa A, Schöttler MA, Kohzuma K, Froehlich JE, Rutherford AW, Satoh-Cruz M, Minhas D, Tietz S, Dhingra A, Kramer DM (2016). Limitations to photosynthesis by proton motive force-induced photosystem II photodamage. *eLife* **5**, e16921.

Davis GA, Rutherford AW, Kramer DM (2017). Hacking the thylakoid proton motive force for improved photosynthesis: modulating ion flux rates that control proton motive force partitioning into Δψ and ΔpH. *Philos Trans R Soc Lond B Biol Sci* **372**, 20160381.

de Bianchi S, Ballottari M, Dall'Osto L, Bassi R (2010). Regulation of plant light harvesting by thermal dissipation of excess energy. *Biochem Soc Trans* **38**, 651–660.

Demmig-Adams B, Cohu CM, Muller O, Adams WW III (2012). Modulation of photosynthetic energy conversion

efficiency in nature: from seconds to seasons. *Photosynth Res* **113**, 75–88.

Duan ZK, Kong FN, Zhang L, Li WJ, Zhang J, Peng LW (2016). A bestrophin-like protein modulates the proton motive force across the thylakoid membrane in *Arabidopsis*. *J Integr Plant Biol* **58**, 848–858.

Duysens LNM (1954). Reversible changes in the absorption spectrum of *Chlorella* upon irradiation. *Science* **120**, 353–354.

Fork DC, Amesz J (1967). Light-induced shifts in the absorption spectrum of carotenoids in red and brown algae. *Photochem Photobiol* **6**, 913–918.

Frese RN, Palacios MA, Azzizi A, van Stokkum IHM, Kruip J, Rögner M, Karapetyan NV, Schlodder E, van Grondelle R, Dekker JP (2002). Electric field effects on red chlorophylls, β-carotenes and P700 in cyanobacterial Photosystem I complexes. *Biochim Biophys Acta Bioenerg* **1554**, 180–191.

Fristedt R, Martins NF, Strenkert D, Clarke CA, Suchoszek M, Thiele W, Schöttler MA, Merchant SS (2015). The thylakoid membrane protein CGL160 supports CF_1CF_o ATP synthase accumulation in *Arabidopsis thaliana*. *PLoS One* **10**, e0121658.

Hind G, Nakatani HY, Izawa S (1974). Light-dependent redistribution of ions in suspensions of chloroplast thylakoid membranes. *Proc Natl Acad Sci USA* **71**, 1484–1488.

Hirano M, Katoh S (1981). Electrochromic band shifts of carotenoid in a blue-green alga. *Photochem Photobiol* **34**, 637–643.

Holmes NG, Hunter CN, Niederman RA, Crofts AR (1980). Identification of the pigment pool responsible for the flash-induced carotenoid band shift in *Rhodopseudomonas sphaeroides* chromatophores. *FEBS Lett* **115**, 43–48.

Joliot P, Joliot A (2002). Cyclic electron transfer in plant leaf. *Proc Natl Acad Sci USA* **99**, 10209–10214.

Junge W, Witt HT (1968). On the ion transport system of photosynthesis: investigations on a molecular level. *Z Naturforsch B* **23**, 244–254.

Klughammer C, Siebke K, Schreiber U (2013). Continuous ECS-indicated recording of the proton-motive charge flux in leaves. *Photosynth Res* **117**, 471–487.

Kramer DM, Avenson TJ, Edwards GE (2004). Dynamic flexibility in the light reactions of photosynthesis governed by both electron and proton transfer reactions. *Trends Plant Sci* **9**, 349–357.

Kramer DM, Cruz JA, Kanazawa A (2003). Balancing the central roles of the thylakoid proton gradient. *Trends Plant Sci* **8**, 27–32.

Kramer DM, Evans JR (2011). The importance of energy balance in improving photosynthetic productivity. *Plant Physiol* **155**, 70–78.

Kramer H, Mathis P (1980). Quantum yield and rate of formation of the carotenoid triplet state in photosynthetic structures. *Biochim Biophys Acta Bioenerg* **593**, 319–329.

Liguori N, Roy LM, Opacic M, Durand G, Croce R (2013). Regulation of light harvesting in the green alga *Chlamydomonas reinhardtii*: the C-terminus of LHCSR is the knob of a dimmer switch. *J Am Chem Soc* **135**, 18339–18342.

Lucker B, Kramer DM (2013). Regulation of cyclic electron flow in *Chlamydomonas reinhardtii* under fluctuating carbon availability. *Photosynth Res* **117**, 449–459.

Nandha B, Finazzi G, Joliot P, Hald S, Johnson GN (2007). The role of PGR5 in the redox poising of photosynthetic electron transport. *Biochim Biophys Acta Bioenerg* **1767**, 1252–1259.

Nawrocki WJ, Santabarbara S, Mosebach L, Wollman FA, Rappaport F (2016). State transitions redistribute rather than dissipate energy between the two photosystems in *Chlamydomonas*. *Nat Plants* **2**, 16031.

Niyogi KK, Grossman AR, Björkman O (1998). *Arabidopsis* mutants define a central role for the xanthophyll cycle in the regulation of photosynthetic energy conversion. *Plant Cell* **10**, 1121–1134.

Pottosin II, Schönknecht G (1996). Ion channel permeable for divalent and monovalent cations in native spinach thylakoid membranes. *J Membr Biol* **152**, 223–233.

Rott M, Martins NF, Thiele W, Lein W, Bock R, Kramer DM, Schöttler MA (2011). ATP synthase repression in tobacco restricts photosynthetic electron transport, CO_2 assimilation, and plant growth by overacidification of the thylakoid lumen. *Plant Cell* **23**, 304–321.

Ruban AV, Pascal AA, Robert B, Horton P (2002). Activation of zeaxanthin is an obligatory event in the regulation of photosynthetic light harvesting. *J Biol Chem* **277**, 7785–7789.

Sacksteder CA, Kanazawa A, Jacoby ME, Kramer DM (2000). The proton to electron stoichiometry of steady-state photosynthesis in living plants: a proton-pumping Q cycle is continuously engaged. *Proc Natl Acad Sci USA* **97**, 14283–14288.

Sacksteder CA, Kramer DM (2000). Dark-interval relaxation kinetics (DIRK) of absorbance changes as a quanti-

tative probe of steady-state electron transfer. *Photosynth Res* **66**, 145–158.

Schmidt S, Reich R, Witt HT (1971). Electrochromism of chlorophylls and carotenoids in multilayers and in chloroplasts. *Naturwissenschaften* **58**, 414.

Schönknecht G, Hedrich R, Junge W, Raschke K (1988). A voltage-dependent chloride channel in the photosynthetic membrane of a higher plant. *Nature* **336**, 589–592.

Schreiber U, Klughammer C (2008). New accessory for the DUAL-PAM-100: the P515/535 module and examples of its application. *PAM Appl Notes* **1**, 1–10.

Sonoike K (2011). Photoinhibition of photosystem I. *Physiol Plant* **142**, 56–64.

Spetea C, Herdean A, Allorent G, Carraretto L, Finazzi G, Szabo I (2017). An update on the regulation of photosynthesis by thylakoid ion channels and transporters in *Arabidopsis*. *Physiol Plant* **161**, 16–27.

Sukhov V, Surova L, Morozova E, Sherstneva O, Vodeneev V (2016). Changes in H^+-ATP synthase activity, proton electrochemical gradient, and pH in *Pea* chloroplast can be connected with variation potential. *Front Plant Sci* **7**, 1092.

Takahashi H, Clowez S, Wollman FA, Vallon O, Rappaport F (2013). Cyclic electron flow is redox-controlled but independent of state transition. *Nat Commun* **4**, 1954.

Takizawa K, Cruz JA, Kanazawa A, Kramer DM (2007). The thylakoid proton motive force *in vivo*. Quantitative, non-invasive probes, energetics, and regulatory consequences of light-induced pmf. *Biochim Biophys Acta Bioenerg* **1767**, 1233–1244.

Tolleter D, Ghysels B, Alric J, Petroutsos D, Tolstygina I, Krawietz D, Happe T, Auroy P, Adriano JM, Beyly A, Cuiné S, Plet J, Reiter IM, Genty B, Cournac L, Hippler M, Peltier G (2011). Control of hydrogen photoproduction by the proton gradient generated by cyclic electron flow in *Chlamydomonas reinhardtii*. *Plant Cell* **23**, 2619–2630.

Viola S, Bailleul B, Yu JF, Nixon P, Sellés J, Joliot P, Wollman FA (2019). Probing the electric field across thylakoid membranes in cyanobacteria. *Proc Natl Acad Sci USA* **116**, 21900–21906.

Wang P, Duan W, Takabayashi A, Endo T, Shikanai T, Ye JY, Mi HL (2006). Chloroplastic NAD(P)H dehydrogenase in tobacco leaves functions in alleviation of oxidative damage caused by temperature stress. *Plant Physiol* **141**, 465–474.

Witt HT (1979). Energy conversion in the functional membrane of photosynthesis. Analysis by light pulse and electric pulse methods: the central role of the electric field. *Biochim Biophys Acta* **505**, 355–427.

Yamori W, Takahashi S, Makino A, Price GD, Badger MR, von Caemmerer S (2011). The roles of ATP synthase and the cytochrome b*6*/*f* complexes in limiting chloroplast electron transport and determining photosynthetic capacity. *Plant Physiol* **155**, 956–962.

Zhang L, Duan ZK, Zhang J, Peng LW (2016). Biogenesis factor required for ATP synthase 3 facilitates assembly of the chloroplast ATP synthase complex. *Plant Physiol* **171**, 1291–1306.

Zhang L, Pu H, Duan ZK, Li YH, Liu B, Zhang QQ, Li WJ, Rochaix JD, Liu L, Peng LW (2018). Nucleus-encoded protein BFA1 promotes efficient assembly of the chloroplast ATP synthase coupling factor 1. *Plant Cell* **30**, 1770–1788.

Zhang R, Cruz JA, Kramer DM, Magallanes-Lundback ME, Dellapenna D, Sharkey TD (2009). Moderate heat stress reduces the pH component of the transthylakoid proton motive force in light-adapted, intact tobacco leaves. *Plant Cell Environ* **32**, 1538–1547.

Zoschke R, Kroeger T, Belcher S, Schöttler MA, Barkan A, Schmitz-Linneweber C (2012). The pentatricopeptide repeat-SMR protein ATP4 promotes translation of the chloroplast *atpB*/*E* mRNA. *Plant J* **72**, 547–558.

The Measurement Principles, Methods and Applications of P515

Chunyan Zhang[1, 2*], Xiaojie Pang[2]

[1]Plant Science Facility of Institute of Botany, Chinese Academy of Sciences, Beijing 100093, China; [2] Key Laboratory of Photobiology, Chinese Academy of Sciences, Beijing 100093, China

Abstract The spectral techniques have been widely used in the field of photosynthesis research, such as the light absorption signals P515 and P700 redox kinetics, and chlorophyll fluorescence, which can detect the photosynthetic activities of plants quickly and accurately. P515 signal is widely present in higher plants and algae, which is caused by the shift of absorption spectrum of pigments on thylakoid membrane. We can detect the ratio of PSI to PSII reaction center, the proton conductivity of chloroplast ATP synthase, the cyclic electron flow rate around PSI, the proton motive force (pmf) and its components by the P515 fast and slow kinetics, and study the photoprotective mechanism by simultaneous detection of P515 signal and chlorophyll fluorescence. In this paper, we summarize the main measurement methods of P515, expound its principles, and the applications. The aim is to provide technical supports for further study on the mechanism of photosynthesis.

Key words P515, ATP synthase, cyclic electron transport, proton motive force

Zhang CY, Pang XJ (2021). The measurement principles, methods and applications of P515. *Chin Bull Bot* **56**, 594–604.

* Author for correspondence. E-mail: zhangchunyan@ibcas.ac.cn

(责任编辑: 朱亚娜)